Infection and Drug Resistance

Dovepress
open access to scientific and medical research

Open Access Full Text Article

ORIGINAL RESEARCH

Microbiological Characteristics of Clinically Isolated *Staphylococcus aureus* with Different Hemolytic Phenotypes in China

Wei Tang[1,2,*], Ying Liu[3,*], Xin Li[2], Guiyun Leng[2], Ju Gao[2], Yawu Wang[2], Jie Yao[2], Zhou Liu[2], Qiang Zhou[2], Yuanhong Xu[1]

[1]Department of Clinical Laboratory, The First Affiliated Hospital of Anhui Medical University, Hefei, 230022, People's Republic of China; [2]Department of Clinical Laboratory, The Second Affiliated Hospital of Anhui Medical University, Hefei, 230601, People's Republic of China; [3]High Magnetic Field Laboratory, Hefei Institutes of Physical Science, Chinese Academy of Sciences, Hefei, 230031, People's Republic of China

*These authors contributed equally to this work

Correspondence: Yuanhong Xu, Department of Clinical Laboratory, The First Affiliated Hospital of Anhui Medical University, 218 Jixi Road, Shushan District, Hefei, Anhui, 230022, People's Republic of China, Tel +86 135 0569 4447, Fax +86 551 6292 2125, Email xyhong1964@ahmu.edu.cn

Purpose: This study aimed to investigate the microbiological characteristics of clinically isolated *Staphylococcus aureus* with different hemolytic phenotypes in China.

Materials and Methods: Using the three-point inoculation method, the hemolytic phenotypes of 1295 clinically isolated *S. aureus* strains were detected and categorized. Antimicrobial susceptibility testing of all strains was performed using a VITEK 2 Compact System. After sample size matching, plasma coagulase activity, catalase activity, mRNA expression of hemolysin genes (*hla, hlb, hlc*, and *hld*), biofilm formation, growth kinetics, inflammatory response of macrophages and cytotoxicity of *S. aureus* with different hemolytic phenotypes using the rabbit plasma kit, the catalase test on slides, qRT-PCR, crystal violet staining, the microcultivation assay, the ELISA kits, and the CCK-8 assay, respectively.

Results: Seven categories of hemolytic phenotypes were identified. Accordingly, strains were categorized into seven different groups, including *S. aureus* with complete hemolytic phenotype (SCHP), *S. aureus* with weak hemolytic phenotype (SWHP), *S. aureus* with incomplete hemolytic phenotype 1 (SIHP-1), SIHP-2, SIHP-3, SIHP-4 and SIHP-5, the last three of which were reported for the first time. Except for the hemolytic phenotype, all seven groups differed in clinical isolation rates, antibiotic resistance profile, plasma coagulase activity, mRNA expression of hemolysin genes, biofilm formation, growth kinetics, inflammatory response of macrophages, and cytotoxicity.

Conclusion: *S. aureus* with different hemolytic phenotypes have distinctive microbiological characteristics. Clinical microbiologists need to be vigilant about the hemolytic phenotypes when culturing *S. aureus* strains, and actively enhance communication with clinicians to optimize the treatment of infection.

Keywords: *Staphylococcus aureus*, hemolytic phenotype, hemolysin, microbiological characteristics, antibiotic resistance

Introduction

Staphylococcus aureus is a global opportunistic pathogen,[1] causing infections ranging from minor skin abscesses to life-threatening septicemia.[2] Of note, methicillin-resistant *S. aureus* (MRSA) is the most clinically important due to its high mortality rate.[3] The pathogenicity of *S. aureus* is determined by several virulence factors, including adherence, colonization, immune evasion, tissue injury, and toxin production. Hemolysin is one of the most important toxins. Specifically, *S. aureus* produces at least four hemolysins, including α-hemolysin, β-hemolysin, γ-hemolysin, and δ-hemolysin. Their combined effects destroy the red blood cell membrane and form the complete transparent hemolytic ring on blood agar plates.[4]

Received: 28 February 2024
Accepted: 10 July 2024
Published: 1 August 2024

Regardless of whether in vivo or in vitro, *S. aureus* frequently encounters sub-minimum inhibitory concentrations (sub-MICs) of antibiotics. This exposure is attributed to a variety of factors, including the misuse of antibiotics, the presence of diffusion barriers, the complexity of pharmacokinetics, the release of waste products, and the use of antibiotics in livestock.[5] Furthermore, *S. aureus* can develop phenotypic changes and even genetic changes to adapt to the stress environments containing sub-MICs of antibiotics.[6] Indeed, different antibiotics have different effects on *S. aureus*.[7] For example, previous studies have shown that sub-MICs of β-lactam antibiotics or fluoroquinolones upregulate the expression of the *hla* gene encoding α-hemolysin, while fusidic acid, clindamycin, macrolides, and aminoglycosides downregulate the expression.[8–10] Additionally, the sub-MICs of ciprofloxacin or trimethoprim can promote the production of β-hemolysin by excising *hlb*-converting prophage.[11] Although there is currently no relevant research, it is reasonable to speculate that γ-hemolysin and δ-hemolysin may also be affected by sub-MICs of antibiotics. Consequently, the actual hemolytic phenotypes of *S. aureus* should probably be diverse, especially for clinically isolated strains. Wherein, *S. aureus* with complete hemolytic phenotype (SCHP) is the most common. In contrast, *S. aureus* with incomplete hemolytic phenotype (SIHP) has only been described in a few studies.[4,12–14] Through a comparative analysis, we have divided the SIHP strains into two distinct categories: SIHP-1 and SIHP-2. On blood agar plates, SIHP-1 was characterized by a single dark and opaque incomplete hemolytic ring surrounding the colony. By comparison, SIHP-2 displayed a dual hemolytic rings phenotype, featuring an inner smaller and transparent complete hemolytic ring encircled by an outer larger and opaque incomplete hemolytic ring. Additionally, the *S. aureus* small colony variant (SCV) has a small, colorless, and weakly hemolytic colony.[15]

In recent years, three novel hemolytic phenotypes of *S. aureus* have been discovered in our hospital, and they are significantly different from the previously known phenotypes. Therefore, elucidating the microbiological characteristics of *S. aureus* strains with different hemolytic phenotypes is of paramount importance for advancing our understanding of their clinical and pathogenic implications. This study reveals that *S. aureus* strains with different hemolytic phenotypes show variations in clinical isolation rates, antibiotic resistance profile, plasma coagulase activity, mRNA expression of hemolysin genes, biofilm formation, growth kinetics, inflammatory response of macrophages, and cytotoxicity.

Materials and Methods

Bacterial Strains and Culture Conditions

After excluding strains from repeated sources, a total of 1295 *S. aureus* strains were isolated from patients at the Second Affiliated Hospital of Anhui Medical University from July 2021 to August 2023. The composition of the departments where the strains were isolated is shown in Table 1. The specimens included 117 blood samples (9.03%), 45 urine samples (3.47%), 80 interstitial fluids samples (6.18%), 442 secretion samples (34.13%), 570 sputa samples (44.02%) and 41 other samples (3.17%).

S. aureus strains were stored in 15% glycerol broth at −80°C and subcultured before being used for any experiment. *S. aureus* strains were grown under shaking at 220 rpm in Luria-Bertani (LB) broth (Sangon Biotech, Shanghai, China) or on Columbia sheep blood agar plates (BAP; Tianda, Hefei, China). The hemolytic phenotype of the bacteria was detected by the three-point inoculation method on BAP which were subsequently incubated at 35°C in an atmosphere containing 5% CO_2 (v/v) for 20 hours and then refrigerated at 4°C for 20 hours, according to the literature method with minor modifications.[4,12] Before and after refrigeration, the changes in the hemolytic zones were photographically recorded. Accordingly, *S. aureus* strains were categorized into 7 groups. The strains were identified as *S aureus* by matrix-assisted laser desorption/ionization time-of-flight mass spectrometry (MALDI-TOF MS; microflex LT; Bruker, Bremen, Germany) and 16S *rRNA* amplicon sequencing. *S. aureus* ATCC29213, *S. aureus* ATCC25923, *Escherichia coli* ATCC25922, and *Staphylococcus epidermidis* acted as quality control strains.

Detection of Hemolytic Phenotype

The hemolytic phenotype was detected by the three-point inoculation method. Firstly, the concentrations of the *S. aureus* strain suspensions were standardized to 3.0×10^8 CFU/mL. Second, each *S. aureus* strain was point-inoculated on the surface of BAP with a spacing of 1.5 cm, forming an equilateral triangle. A volume of 0.5 μL suspension was applied per point. Thirdly, the plates were allowed to dry on a laminar flow bench for 10 minutes. Fourthly, the plates were incubated

Table 1 Constituent Ratios of Departments Where Strains Were Isolated

Department	Strains, n (%)
Neurology	71 (5.48)
Orthopedic	88 (6.80)
Pediatrics	57 (4.40)
Gastroenterology	12 (0.93)
Out-patient	25 (1.93)
Infectious diseases	57 (4.40)
Oncology	37 (2.86)
Intensive Care Unit	307 (23.71)
General surgery	79 (6.10)
Respiration	81 (6.25)
Plastic surgery	68 (5.25)
Cerebral surgery	49 (3.78)
Urology	25 (1.93)
Endocrinology	53 (4.09)
Dermatology	28 (2.16)
Hematology	57 (4.40)
Nephrology	63 (4.86)
Obstetrics and Gynecology	28 (2.16)
Cardiology	23 (1.78)
Cardiovascular Surgery	23 (1.78)
Rheumatism and Immunological Disease	17 (1.31)
Others	47 (3.63)
Total	1295 (100.00%)

at 35°C in an atmosphere containing 5% CO_2 (v/v) for 20 hours. Finally, the plates were refrigerated at 4°C for 20 hours. The resulting hemolytic zones around the colonies were photographically recorded. The *S. aureus* strains were then categorized into distinct groups based on the changes observed in the hemolytic zones.

Antimicrobial Susceptibility Testing

Based on the broth microdilution method and the Clinical and Laboratory Standards Institute guidelines (CLSI M100-S29), antimicrobial susceptibility testing of *S. aureus* strains was performed using a VITEK 2 Compact System and a VITEK 2 AST-GP639 test kit (bioMerieux, Inc., Durham, NC, USA). Fifteen antibiotics were tested, including penicillin (PEN), oxacillin (OXA), gentamicin (GEN), rifampicin (RIF), levofloxacin (LVX), moxifloxacin (MFX), erythromycin (ERY), clindamycin (CLI), daptomycin (DAP), trimethoprim/sulfamethoxazole (SXT), linezolid (LNZ), vancomycin (VAN), teicoplanin (TEC), tigecycline (TGC), and ceftaroline (CTL). The MRSA status was determined using the minimum inhibitory concentration (MIC) of two antibiotics: oxacillin MIC >4 μg/mL, and cefoxitin MIC >8 μg/mL. Furthermore, the cefoxitin (30 μg) disk diffusion test was performed on the Mueller-Hinton agar plate (MH; Tianda, Hefei, China) and incubated at 37°C for 18 hours to verify MRSA.

Detection of Plasma Coagulase Activity

The coagulase test was performed with rabbit plasma (Catalog No. HB4117-4, Hopebio, Qingdao, China). Each vial containing freeze-dried rabbit plasma was supplemented with 800 μL of an overnight bacterial culture. The mixture was gently mixed until completely dissolved and then incubated at 37°C. Monitored the outcomes at 30-minute intervals for a continuous period of 6 hours. If a clot was observed when the vial was tilted or inverted, a positive result was recorded. Otherwise, with continued observation for 24 hours, the non-clotting test was considered negative. Based on the clot volume (V_{clot}) and the original volume ($V_{original}$), the intensity of the plasma coagulase reaction was categorized as

negative reaction (no clot was observed), weak reaction ($V_{clot} < 1/2\ V_{original}$), moderate reaction ($1/2\ V_{original} \leq V_{clot} < V_{original}$) or strong reaction ($V_{clot} = V_{original}$).

Detection of Catalase Activity

The catalase activity of *S. aureus* with different hemolytic phenotypes was detected by slide catalase test with 3% (v/v) hydrogen peroxide. In brief, the visibility of effervescence confirmed the catalase-positive test for this strain. Conversely, no effervescence confirmed a negative catalase test.

Extraction of RNA

The bacteria were grown overnight on BAP. Sterile disposable plastic loops were used to transfer an appropriate number of colonies into 2-mL polypropylene snap-cap liquid nitrogen grinding tubes (Jingxin, Shanghai, China). Each contained 1 mL of sterile double-distilled water. The bacterial pellets were collected by centrifugation at 15 000g for 5 minutes. Subsequently, the grinding tubes were quickly immersed in liquid nitrogen and ground for 5 minutes using a freeze grinder (Jingxin, Shanghai, China). After grinding, the tubes were stored at −80°C.

An RNA extraction kit (Catalog No. B518625, Sangon Biotech, Shanghai, China) was used to extract total RNA. According to the instructions of the kit and the protocol of Cold Spring Harbor Laboratory Press,[16] the quantity and quality of extracted RNA were determined by spectrophotometry using the NanoDrop spectrophotometer (Thermo Fisher Scientific, MA, USA). Subsequently, residual DNA was removed and complementary DNA (cDNA) was synthesized using a ToloScript RT EasyMix kit (Catalog No. 22106, TOLO Biotech, Shanghai, China) with gDNA eraser. cDNA products were stored at −80°C until further analysis.

Detection of the mRNA Levels of Four Hemolysin Genes

Specific primers were designed using the NCBI Primer-BLAST. cDNA from five strains of each group was used as a template for quantitative real-time PCR (qRT-PCR) and the specific primers were shown in Table 2. Briefly, qRT-PCR was performed using a SYBR Green Master mix kit (Catalog No. 22204, TOLO Biotech, Shanghai, China). The reaction conditions were as follows: pre-denaturation at 95°C for 30 seconds, followed by 40 cycles of 10s at 95 °C, and 30s at 60 °C. Reactions were performed in a MicroAmp Optical 96-well reaction plate using QuantStudio 5 (Applied Biosystems™, Thermo Fisher Scientific, MA, USA). Cycling thresholds (Ct) were determined by automated threshold analysis. All qRT-PCR assays were repeated three times. Messenger RNA (mRNA) levels of four hemolysin genes (*hla, hlb, hlc*, and *hld*) were calculated by normalizing to the housekeeper gene *gyrB* (DNA gyrase subunit B). The data were analyzed using the $2^{-\Delta\Delta Ct}$ method.

Biofilm Crystal Violet Staining

The biofilm formation was detected using the crystal violet (CV) staining method, which provided a semi-quantitative measurement of biofilm formation, as described previously.[17] Briefly, overnight cultures were diluted in LB broth to

Table 2 Primers Used in This Study

Primer name	GenBank Number	Primer Sequences (5'-3')	Product Size	Primer Source
hla-F	KT279561	TGGTTTAGCCTGGCCTTCAG	190 bp	This study
hla-R		ATTTGCACCAATAAGGCCGC		
hlb-F	EF690812	GGGGCAATATAAACGCGCTG	167 bp	This study
hlb-R		CTGATTGAGAACGGCCGAGT		
hlc-F	D42143	TTGCACAAGACCCAACTGGT	173 bp	This study
hlc-R		AGCATCCATGTTTCTGCCGT		
hld-F	AB043555	GGAAGGAGTGATTTCAATGGCA	88 bp	This study
hld-R		AGTGAATTTGTTCACTGTGTCG		
gyrB-F	M86227	ACGAAGGTGGTACGCATGAA	278 bp	This study
gyrB-R		TGTACGTGCGACTTGTGGAT		

obtain a final concentration of 1.0×10^6 CFU/mL. The diluted cultures (200 μL/well) were aliquoted into a 96-well flat-bottom microplate (Costar, Corning, ME, USA). Biofilms were allowed to grow for 36 hours at 37°C. Thereafter, the supernatant was removed from each well and washed three times with water to remove loosely adherent bacteria. Afterward, 200 μL of 2.5% glutaraldehyde was added to each well for 30 minutes to fix the biofilm. The wells were washed with water after the fixative was carefully aspirated. Then, 200 μL of 0.2% (wt/vol) CV solution was added to each well and stained for 15 minutes. After removal of the CV solution, the biofilms were washed with water until the removed liquid appeared clear. Subsequently, 200 μL of 30% acetic acid solution was added to each well for 20 minutes to allow the dye that had entered the biofilm to dissolve completely. To quantify biofilm formation, the absorbance at 585 nm was measured using a microplate spectrophotometer (Spectra max i3x, Molecular Devices, CA, USA). Five biological replicates were analyzed for each strain. The optical density (OD_{585}) values from the wells that had not been inoculated with bacteria were used as negative controls. In accordance with a previous study, the cut-off value for optical density (ODc) to determine a biofilm producer was defined as twice the value of the negative control.[18] Based on the OD_{585} values, the strains were categorized as non-biofilm producers ($OD_{585} < ODc$), weak biofilm producers ($ODc \leq OD_{585} < 2ODc$) or strong biofilm producers ($OD_{585} \geq 2ODc$).

Growth Kinetic Assays

Except for *S. aureus* ATCC29213 and *S. aureus* ATCC25923, the growth kinetics of 5 strains in each group were tested through the microcultivation assay as previously described.[19] Briefly, the log-phase bacteria were centrifuged and resuspended with fresh LB broth medium to get a starting concentration of 1.0×10^6 CFU/mL. Subsequently, 200 μL of bacterial suspension was transferred to each well of Costar clear polystyrene 96-well flat-bottom microplate (Corning, ME, USA). Two biological replicates were analyzed for each strain. Then, the microplate was incubated at 37 °C. Bacterial growth kinetics was recorded for 30.5 hours by measuring the OD_{600}, using a microplate spectrophotometer (Spectra max i3x, Molecular Devices, CA, USA). The data were analyzed using the Origin 2021 software (Origin Lab Corporation, Northampton, MA, USA) to generate growth curves.

Quantification of Cytokines Secretion from *S. aureus* Stimulated Macrophages

The culture supernatants of mouse macrophage RAW264.7 cells stimulated by *S. aureus* strains were collected. The levels of cytokines (IL-1β, IL-6, and TNF-α) were determined by using ELISA kits (Catalog No. CSB-E08054m, CSB-E04639m, CSB-E04741m; Cusabio, Wuhan, China) according to the manufacturer's instructions. Briefly, cells (1.0×10^5 cells/mL, complete RPMI 1640 medium) were seeded in a 48-well Transwell plate (Costar, Corning, ME, USA), 1 mL per well, followed by incubation with 100 μL of LB broth or logarithmic phase bacteria (1.8×10^8 CFU/mL) at 37°C for 24 hours. Then, the plate was centrifuged and the supernatant was collected. Successively, three 100 μL aliquots of each supernatant were taken to determine the concentrations of cytokines. Finally, the absorbance was measured at 450 nm using a microplate spectrophotometer (Spectra max i3x, Molecular Devices, CA, USA).

Cytotoxicity Assay

The cytotoxicity of *S. aureus* strains on mouse macrophage RAW264.7 cells (ATCC, Manassas, VA, USA) was evaluated by cell counting kit-8 (CCK8; Catalog No. C0037, Beyotime Biotech, Shanghai, China) assay according to the instructions. Briefly, cells (1×10^5 cells/mL) were seeded in a 48-well Transwell plate (Costar, Corning, ME, USA), 1 mL per well, followed by incubation with 100 μL of LB broth or logarithmic phase bacteria (1.8×10^8 CFU/mL) at 37°C for 24 hours. Then, the plate was centrifuged and the supernatant was discarded. Successively, 40 μL of CCK-8 solution was mixed with 400 μL of Dulbecco's modified Eagle's medium (DMEM) containing 10% fetal calf serum, added into each well, and incubated in the dark for 1 hour. Finally, the absorbance was measured at 450 nm using a microplate spectrophotometer (Spectra max i3x, Molecular Devices, CA, USA). The media without cells and bacteria was a blank control.

$$\text{Cell viability}\,(\%) = (OD_{\text{bacteria}} - OD_{\text{blank}})/(OD_{\text{LB}} - OD_{\text{blank}}) \times 100\%.$$

Statistical Analyses

One-way ANOVA, *Kruskal–Wallis*, and Chi-squared test were used for the statistical analysis. Error bars on the figures represent standard deviations (SD) of the mean. Statistical significance was defined as $P < 0.05$. All the statistical analyses were performed using SPSS 18.0 software (SPSS Inc., USA).

Results

Novel Hemolytic Phenotypes of *S. aureus* Strains on Sheep Blood Agar Plates

According to the morphological characteristics of the hemolytic ring around the colony, a total of 7 hemolytic phenotypes of *S. aureus* were categorized in the study, including SCHP, *S. aureus* with weak hemolytic phenotype (SWHP), and 5 subtypes of SIHP (SIHP-1, SIHP-2, SIHP-3, SIHP-4, and SIHP-5). Among the 1295 clinical isolates, 1036 (80.00%) strains were classical SCHP, 42 (3.24%) strains were SWHP, 20 (1.54%) strains were SIHP-1, 25 (1.93%) strains were SIHP-2, 26 (2.00%) strains were SIHP-3, 136 (10.50%) strains were SIHP-4, and 10 (0.77%) strains were SIHP-5.

For classical SCHP, a transparent complete hemolytic ring (Φ=12.0 ± 0.3 mm) with a hazy edge (Φ=19.6 ± 0.9 mm) was observed around the colony (Figure 1A). For SWHP, almost no visible hemolytic ring was observed around the colony (Figure 1B). For SIHP-1, a dark and opaque incomplete hemolytic ring (Φ=11.1 ± 0.3 mm) was observed around the colony (Figure 1C). For SIHP-2, an inner smaller and transparent complete hemolytic ring (Φ=7.7 ± 0.4 mm) encircled by an outer larger and opaque incomplete hemolytic ring (Φ=18.1 ± 0.7 mm) was observed around the colony (Figure 1D). For SIHP-3, a big translucent incomplete hemolytic ring (Φ=20.0 ± 0.6 mm) was observed around the colony (Figure 1E). For SIHP-4, an inner smaller and transparent complete hemolytic ring (Φ=8.2 ± 0.3 mm) encircled by an outer larger and translucent incomplete hemolytic ring (Φ=18.6 ± 0.4 mm) was observed around the colony (Figure 1F). For SIHP-5, before refrigeration, the dual hemolytic rings phenotype resembled SIHP-4; however, after refrigeration, an almost transparent incomplete hemolytic ring (Φ=22.0 ± 0.3 mm) emerged on the outer ring (Φ=17.6 ± 0.1 mm) (Figure 1G). Additionally, ATCC29213 (Figure 1H) and ATCC25923 (Figure 1I) were similar to SCHP and SIHP-2, respectively. Interestingly, for all 5 subtypes of SIHP, a transparent linear hemolytic enhanced zone formed at the junction of the two neighboring incomplete hemolytic rings.

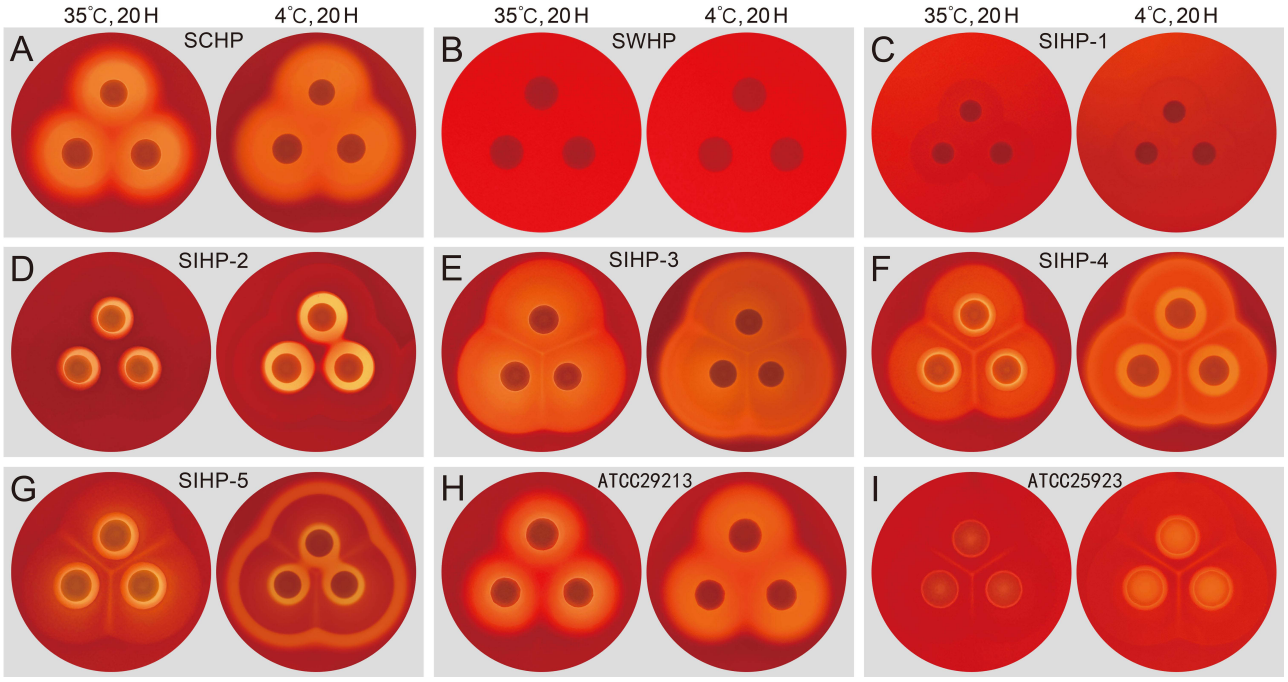

Figure 1 Hemolytic phenotype comparative analysis of *S. aureus* on sheep blood agar plates.
Notes: (**A**) *S. aureus* with complete hemolytic phenotype (SCHP, n = 1036). (**B**) *S. aureus* with weak hemolytic phenotype (SWHP, n = 42). (**C**) *S. aureus* with incomplete hemolytic phenotype 1 (SIHP-1, n = 20). (**D**) *S. aureus* with incomplete hemolytic phenotype 2 (SIHP-2, n = 25). (**E**) *S. aureus* with incomplete hemolytic phenotype 3 (SIHP-3, n = 26). (**F**) *S. aureus* with incomplete hemolytic phenotype 4 (SIHP-4, n = 136). (**G**) *S. aureus* with incomplete hemolytic phenotype 5 (SIHP-5, n = 10). (**H**) *S. aureus* ATCC29213. (**I**) *S. aureus* ATCC25923.

Antibiotic Resistance of *S. aureus* Strains

The antibiotic resistance profile of *S. aureus* with different hemolytic phenotypes was demonstrated in Figure 2. It shows that *S. aureus* strains presented high resistance to PEN (91.20%), OXA (38.07%), ERY (47.26%), and CLI (44.86%) when compared with the other antibiotics tested such as LVX (10.81%), MFX (8.88%), GEN (4.25%), DAP (1.24%), RIF (0.46%), SXT (6.49%), LZD (0.00%), VAN (0.00%), TEC (0.00%), TGC (0.00%), and CTL (0.00%).

For *S. aureus* with different hemolytic phenotypes, antibiotic resistance was observed most frequently to PEN. All SWHP and SIHP-5 were resistant to PEN (100%). Statistical analysis showed that SCHP has significantly lower resistance rates to OXA (32.14%) than SIHP-1 (80.00%), SIHP-2 (64.00%), SIHP-4 (67.65%), and SIHP-5 (80.00%); lower resistance rates to GEN (3.57%) than SIHP-3 (23.08%); lower resistance rates to LEV (8.98%) and MXF (7.14%) than SIHP-1 (35.00% and 30.00%, respectively) and SIHP-3 (both 34.62%); lower resistance rates to ERY (44.40%) and CLI (41.60%) than SIHP-4 (60.29% and 58.09%, respectively). Similarly, SWHP has significantly lower resistance rates to OXA (38.10%) and ERY (33.33%) than SIHP-1 and SIHP-4. In addition, SIHP-3 has significantly higher resistance rates to GEN and SXT (19.23%) than SIHP-4 (2.94% and 2.21%, respectively).

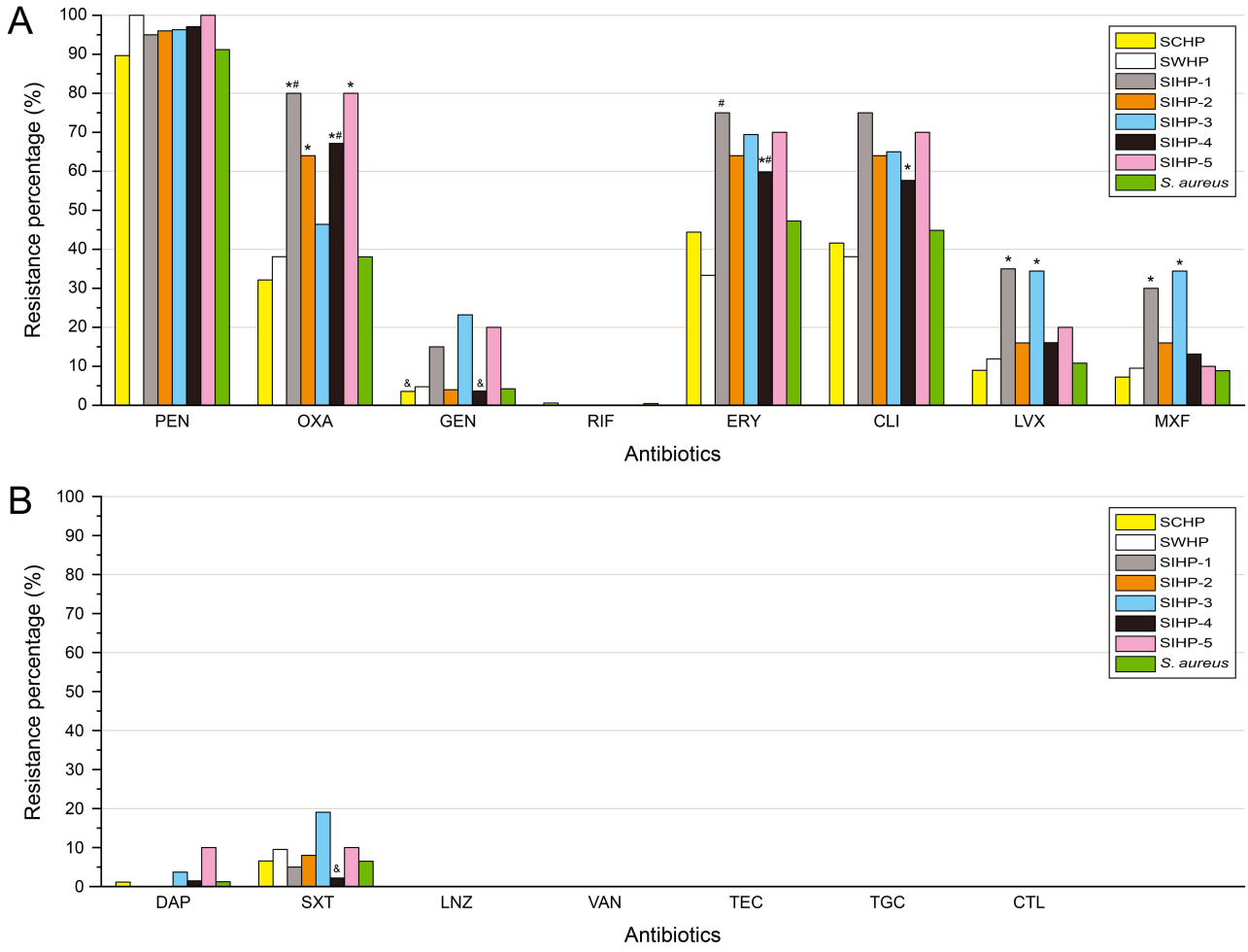

Figure 2 Antibiotic resistance profile of 1295 *S. aureus* with different hemolytic phenotypes.

Notes: (**A**) Antimicrobial characteristics of *S. aureus* with different hemolytic phenotypes in terms of 8 antibiotics. (**B**) Antimicrobial characteristics of *S. aureus* with different hemolytic phenotypes in terms of 7 antibiotics. *Statistically significant versus *S. aureus* with complete hemolytic phenotype (SCHP); #Statistically significant versus *S. aureus* with weak hemolytic phenotype (SWHP); &Statistically significant versus *S. aureus* with incomplete hemolytic phenotype 3 (SIHP-3).

Abbreviations: CLI, clindamycin; CTL, ceftaroline; DAP, daptomycin; ERY, erythromycin; GEN, gentamicin; LNZ, linezolid; LVX, levofloxacin; MFX, moxifloxacin; OXA, oxacillin; PEN, penicillin; RIF, rifampicin; SXT, trimethoprim/sulfa-methoxazole; TEC, teicoplanin; TGC, tigecycline; VAN, vancomycin.

Plasma Coagulase Activity of *S. aureus* Strains

Considering the huge differences in the number of *S. aureus* with different hemolytic phenotypes, 5 strains were randomly selected from each group for the detection of plasma coagulase activity. In SCHP, 2 negative reactions, and 1 weak reaction. In SIHP-2, 2 moderate reactions. In SIHP-3, 1 moderate reaction. In SIHP-5, 1 weak reaction. The rest *S. aureus* was all strong reaction.

Catalase Activity of *S. aureus* Strains

The catalase activity of *S. aureus* with different hemolytic phenotypes was positive and there was no difference in activity intensity.

Relative mRNA Expression Levels of Four Hemolysin Genes

Fold changes of four hemolysin genes (*hla, hlb, hlc*, and *hld*) expression were calculated using the $2^{-\Delta\Delta Ct}$ method. Data represented *gyrB*-normalized target gene expression level relative to that in *S. aureus* ATCC25923 which was considered 1. As shown in Figure 3, the transcriptional expression levels of four hemolysin genes among *S. aureus* with different

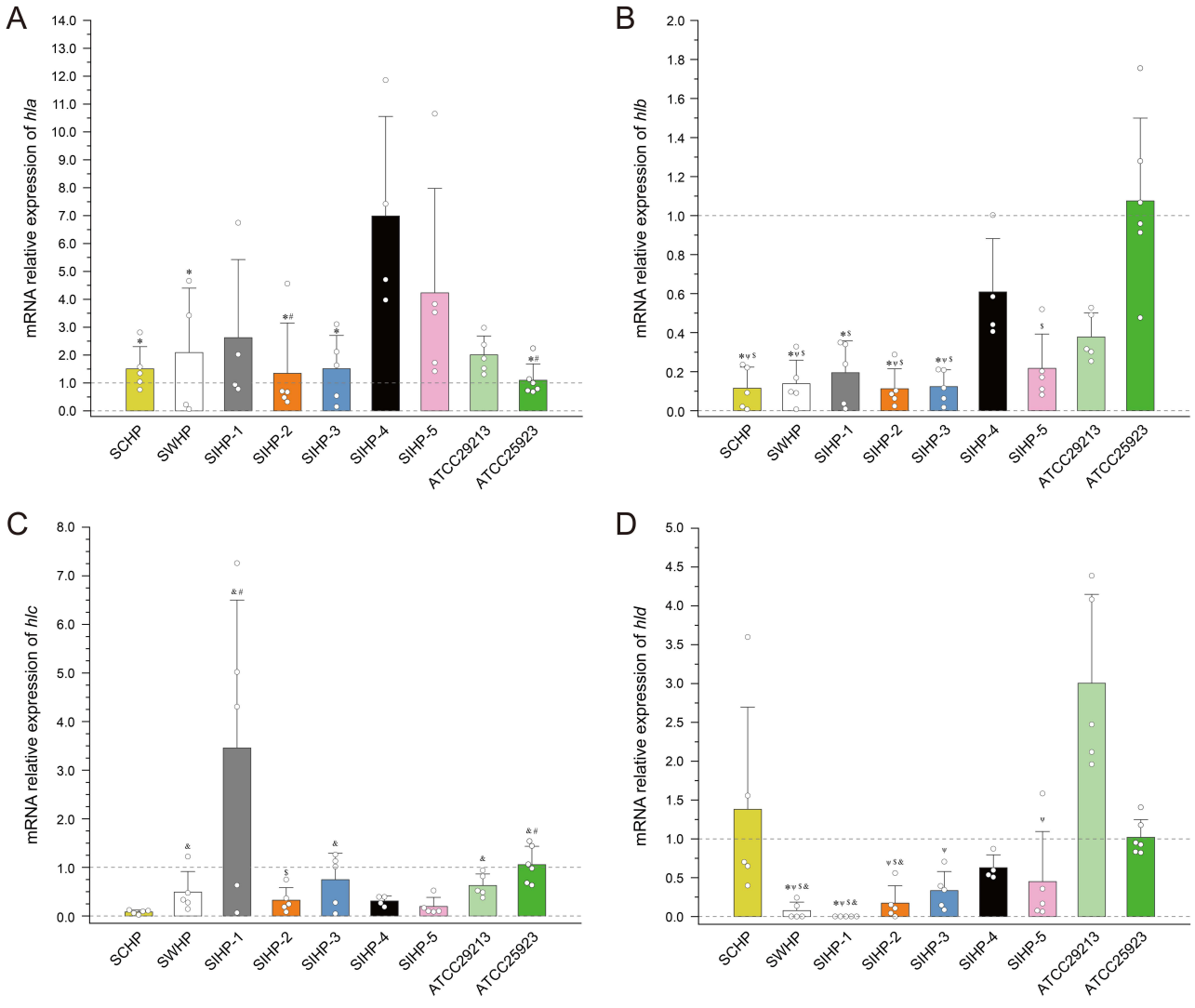

Figure 3 Comparison of the transcriptional expression levels of four hemolysin genes among *S. aureus* with different hemolytic phenotypes.

Notes: (**A**) Transcriptional expression levels of *hla*. (**B**) Transcriptional expression levels of *hlb*. (**C**) Transcriptional expression levels of *hlc*. (**D**) Transcriptional expression levels of *hld*. Bars indicate the standard deviations from the mean. [&]Statistically significant versus *S. aureus* with complete hemolytic phenotype (SCHP); *Statistically significant versus *S. aureus* with incomplete hemolytic phenotype 4 (SIHP-4); [#]Statistically significant versus *S. aureus* with incomplete hemolytic phenotype 5 (SIHP-5); [ψ]Statistically significant versus *S. aureus* ATCC29213; [$]Statistically significant versus *S. aureus* ATCC25923.

hemolytic phenotypes were significantly different (*Kruskal–Wallis* test: *hla, P* = 0.036; *hlb, P* < 0.001; *hlc, P* = 0.005; and *hld, P* < 0.001). The detailed results are described below. Firstly, as for *hla*, SIHP-4 was significantly increased 7.0-folds to ATCC25923, 4.6-folds to SCHP, 3.3-folds to SWHP, 5.2-folds to SIHP-2, and 4.6-folds to SIHP-3. Moreover, SIHP-5 significantly increased by 4.2-folds to ATCC25923, and 3.1-folds to SIHP-2. Secondly, as for *hlb*, SIHP-4 was significantly increased 5.3-folds to SCHP, 4.4-folds to SWHP, 3.1-folds to SIHP-1, 5.4-folds to SIHP-2, and 4.9-folds to SIHP-3. Furthermore, SCHP, SWHP, SIHP-1, SIHP-2, SIHP-3, and SIHP-5 were significantly suppressed by 8.7-, 7.2-, 5.1-, 8.9-, 8.1-, and 4.6-folds compared with ATCC25923. Similarly, SCHP, SWHP, SIHP-2, and SIHP-3 were significantly suppressed by 3.3-, 2.7-, 3.4-, and 3.1-folds compared with ATCC25913. Thirdly, as for *hlc*, SCHP was significantly suppressed by 6.0-folds to SWHP, 42.1-folds to SIHP-1, 9.1-folds to SIHP-3, 7.6-folds to ATCC29213, and 12.9-folds to ATCC25923. Additionally, SIHP-5 was significantly suppressed by 17.7- and 5.4-folds compared with SIHP-1 and ATCC25923. Similarly, SIHP-2 was significantly suppressed by 3.2-folds compared with ATCC25923. Fourthly, as for *hld*, ATCC29213 was significantly increased 39.6-folds to SWHP, 3196.7-folds to SIHP-1, 17.5-folds to SIHP-2, 9.0-folds to SIHP-3, and 6.7-folds to SIHP-5. In comparison, ATCC25923 significantly increased 13.4-folds to SWHP, 1084.6-folds to SIHP-1, and 5.9-folds to SIHP-2. Then, SCHP significantly increased 18.2-folds to SWHP, 1469.1-folds to SIHP-1, and 8.0-folds to SIHP-2. Further, SIHP-4 significantly increased 8.3-folds to SWHP and 668.4-folds to SIHP-1.

Biofilm Formation Analysis

Based on the OD_{585} values, SIHP-1 and SIHP-3 were defined as strong biofilm producers; the rest were defined as weak biofilm producers. Statistical results are as follows. SIHP-1 was significantly increased 2.4-folds to SCHP, 1.5-folds to SWHP, 1.8-folds to SIHP-2, 1.8-folds to SIHP-4, 2.1-folds to SIHP-5, and 1.9-folds to ATCC25923. Similarly, SIHP-3 was significantly increased by 2.0-folds to SCHP, 1.8-folds to SIHP-5, and 1.6-folds to ATCC25923. In addition, ATCC29213 significantly increased 1.7-folds to SCHP and 1.5-folds to SIHP-5. By contrast, SCHP was significantly suppressed by 1.6-folds to SWHP, and 1.3-folds to SIHP-4. See Figure 4 for further details.

Growth Kinetic Characteristics

The bacterial growth kinetic experiment showed differential growth rates among *S. aureus* strains with different hemolytic phenotypes. However, SCHP, SWHP, and SIHP-1 exhibited relatively similar growth kinetics to some degree, because the log and stationary phase growths in the three cultures appeared comparable. The log phase growths of SIHP-2, SIHP-3, SIHP-5, and ATCC29213 were earlier than the above three *S. aureus* with different hemolytic phenotypes. Furthermore, the stationary phase growths of SIHP-5 and ATCC29213 were about 1.4-folds to the above three. Although the log phase growth of ATCC25923 was delayed, the stationary phase growth approached SIHP-5 and was second only to ATCC29213. It is noteworthy that, for SIHP-3 and SIHP-4, there was a crossover between the two log phase growths, resulting in a higher number of bacteria in the stationary phase of the latter. See Figure 5 for further details.

Inflammatory Response of Macrophages to *S. aureus* Strains

To compare the inflammatory responses of macrophages stimulated by *S. aureus* with different hemolytic phenotypes, we examined the pro-inflammatory cytokines in the culture supernatants. See Figure 6 for further details. Roughly speaking, *S. aureus* strains could stimulate macrophages to secrete pro-inflammatory cytokines, including IL-1β (Figure 6A), IL-6 (Figure 6B), and TNF-α (Figure 6C). Specifically, first, SIHP-1 had significantly higher levels of IL-1β than SWHP, ATCC29213, and ATCC25923. Second, SIHP-1, SIHP-2, SIHP-3, SIHP-4, and SIHP-5 had higher levels of IL-6 than SCHP, SWHP, and ATCC25923. Moreover, SIHP-1, SIHP-2, and SIHP-3 had higher levels of IL-6 than ATCC29213. Third, SIHP-5 had higher levels of TNF-α than SWHP and SIHP-2. Besides, SIHP-2 had lower levels of TNF-α than SIHP-1 and SIHP-3.

Cytotoxicity Assay

The CCK-8 assay revealed statistically significant higher OD_{450} values of LB control compared with SCHP, SIHP-1, SIHP-2, and SIHP-4. In addition, SIHP-1 had statistically significantly lower OD_{450} values compared with SWHP and

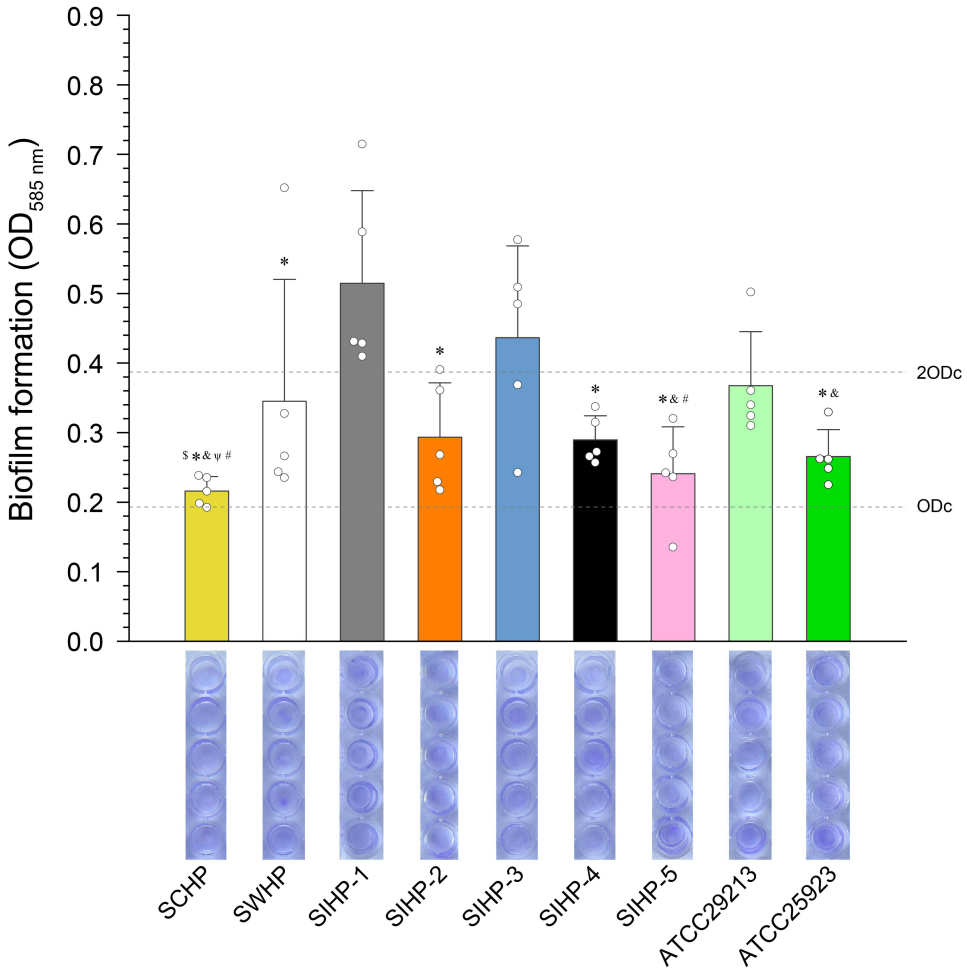

Figure 4 Biofilm formation of *S. aureus* with different hemolytic phenotypes was analyzed by crystal violet (CV) staining method.
Notes: Mean values from five biological replicates are shown. Bars indicate the standard deviations from the mean. [$]Statistically significant versus *S. aureus* with weak hemolytic phenotype (SWHP); [*]Statistically significant versus *S. aureus* with incomplete hemolytic phenotype 1 (SIHP-1); [&]Statistically significant versus *S. aureus* with incomplete hemolytic phenotype 3 (SIHP-3); [ψ]Statistically significant versus *S. aureus* with incomplete hemolytic phenotype 4 (SIHP-4); [#]Statistically significant versus ATCC29213.
Abbreviations: ODc, cut-off optical density value.

SIHP-3. The results showed that SCHP, SIHP-1, SIHP-2, and SIHP-4 exhibited obvious cytotoxic effects on mouse macrophage RAW264.7 cells, reducing cell proliferation activity. Among them, SIHP-1 seemed to have the stronger cytotoxicity. See Figure 7 for further details.

Discussion

The present study revealed that *S. aureus* was found to have at least 7 hemolytic phenotypes, including SCHP, SWHP, SIHP-1, SIHP-2, SIHP-3, SIHP-4, and SIHP-5. To our knowledge, the latter three cannot be classified into any known subtypes of SIHP, and they were defined for the first time. *S. aureus* strains with different hemolytic phenotypes show variations in clinical isolation rates, antibiotic resistance profile, plasma coagulase activity, mRNA expression of hemolysin genes, biofilm formation, growth kinetics, inflammatory response of macrophages, and cytotoxicity. Not surprisingly, all *S. aureus* strains tested positive for catalase activity. This also reflects the fact that the genes controlling catalase synthesis are more conserved and stable compared to those controlling plasma coagulase synthesis.

In this study, 3.24% of strains were SWHP, 1.54% were SIHP-1, 1.93% were SIHP-2, 2.00% were SIHP-3, 10.50% were SIHP-4, and 0.77% were SIHP-5. Consistent with previous studies,[4,13,14] the overwhelming majority of clinically isolated *S. aureus* strains were classical SCHP. By contrast, previous studies have shown that 22.60% of clinical strains

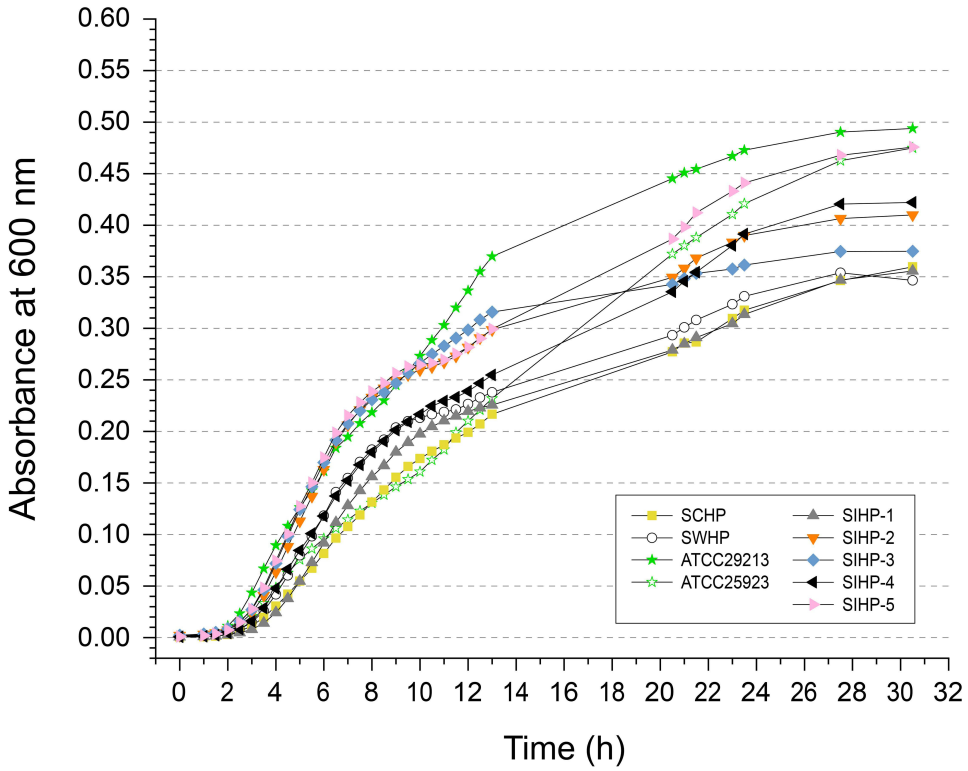

Figure 5 Growth kinetics of *S. aureus* with different hemolytic phenotypes.

were SWHP,[20] 24.62% were SIHP-2,[14] and no data was provided for SIHP-1.[4] Notably, besides weak hemolytic phenotype, the colony morphology and growth properties of SWHP included were different from previously reported *S. aureus* SCV.[21] Hemolytic toxins of *S. aureus* can damage many mammalian cells. Normally, a bright and transparent complete hemolytic zone with a blurred edge around the colony on sheep BAP is suggested to be caused by α-hemolysin, whereas a dark and opaque incomplete hemolytic zone with a sharp edge is considered due to β-hemolysin. Furthermore, dark and opaque incomplete hemolytic zone with blurred edge is considered due to δ-hemolysin. However, γ-hemolysin cannot lead to any visible hemolytic zone. Remarkably, β-hemolysin is a hot-cold hemolysin with a sphingomyelinase and a biofilm ligase activity. Thus, the hemolytic activity of β-hemolysin-producing *S. aureus* could be enhanced by incubation on BAP at 35°C or 37°C, followed by cooling to 4°C. In addition, Wang et al reported that β-hemolysin can partially inhibit the hemolytic activity of α-hemolysin, but strongly reinforce the hemolytic activity of δ-hemolysin, resulting in a narrower turbid zone and a visible transparent complete hemolytic zone, respectively.[22] As demonstrated in this study, *S. aureus* with different hemolytic phenotypes have distinct transcriptional expression profiles of four hemolysin genes, which may be the direct reason for the emergence of novel hemolytic phenotypes.

Attention must be paid to the situation in which β-hemolysin is variably produced by *S. aureus*, depending on the presence or absence of *hlb*-converting prophage whose insertion inactivates *hlb*.[23] The prophage has been found in about 90% of human clinical isolates, but only about 30% of animal isolates.[24] However, the excision of the prophage could be promoted by chronic infections, oxidative stress, antibiotics, and temperature changes, increasing the production of β-hemolysin.[11,25] In addition to its well-known hemolytic activity towards erythrocytes, β-hemolysin could also worsen infections of bovine mammary glands and keratitis in rabbits, promote neutrophilic inflammation and the vascular leakage of serum proteins, and play an important role in skin colonization by damaging keratinocytes.[26,27] Indeed, as shown in this study, SIHP-4 had a relatively higher level of β-hemolysin compared to the overwhelming majority of other *S. aureus*. Interestingly, a transparent linear hemolytic enhanced zone formed between the two neighboring colonies of each SIHP subtype. A few previous studies have also discovered such zone,[4,12–14] which is probably formed by

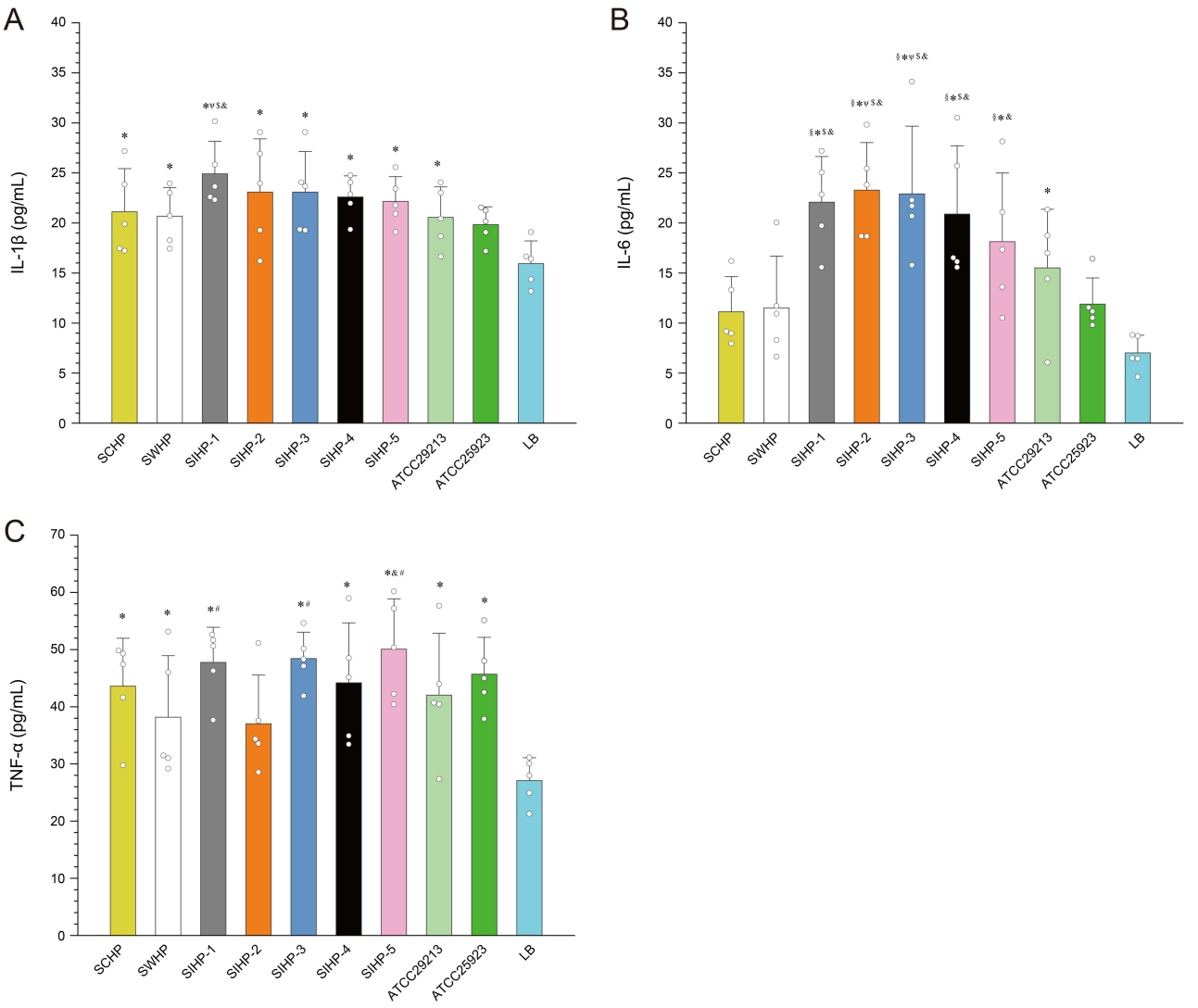

Figure 6 Detection of cytokines secreted by macrophages stimulated with *S. aureus*.

Notes: (**A**) *S. aureus* strains stimulate macrophages to secrete IL-1β. (**B**) *S. aureus* strains stimulate macrophages to secrete IL-6. (**C**) *S. aureus* strains stimulate macrophages to secrete TNF-α. The mean and standard deviations of five biological replicates are shown. *Statistically significant versus Luria-Bertani (LB) broth control; [¥]Statistically significant versus *S. aureus* ATCC29213; [$]Statistically significant versus *S. aureus* ATCC25923; [§]Statistically significant versus *S. aureus* with complete hemolytic phenotype (SCHP); [&]Statistically significant versus *S. aureus* with weak hemolytic phenotype (SWHP); [#]Statistically significant versus *S. aureus* with incomplete hemolytic phenotype 2 (SIHP-2).

Abbreviations: IL-1β, cytokines interleukin 1β; IL-6, cytokines interleukin 6; TNF-α, tumor necrosis factor α.

a mechanism similar to the precipitation line in counter immunoelectrophoresis. Specifically, β-hemolysins secreted by two neighboring colonies met at the appropriate site, causing enhanced hemolysis.

Except for hemolytic toxins, *S. aureus* also produces other kinds of exotoxins, exoenzymes, cell surface-associated antigens, and antibiotic resistance-related molecules. The regulation of these factors in is mediated by a complex network that integrates environmental signals and host signals. In general, the regulatory systems include the two-component systems (AgrAC, SaeRS, SrrAB, and ArlRS), the cytoplasmic SarA-family regulators (SarA, MgrA, and Rot), and the alternative sigma factors (SigB and SigH). They work together to affect the adhesion, colonization, antibiotic resistance profile, immune evasion, intercellular interactions, and tissue injury capacity of *S. aureus*. Of these, the two-component systems are particularly important. Briefly, membrane-associated histidine kinase can be activated by external signals, causing its autophosphorylation and subsequent phosphorylation of response regulators. Upon phosphorylated, the response regulator binds to specific DNA sequence motifs and alters target gene expression.[28] Among the two-component systems, the best studied is the accessory gene regulator (*agr*), which plays a central role in pathogenesis, senses external signals through auto-induced peptide, and encodes a quorum-sensing system

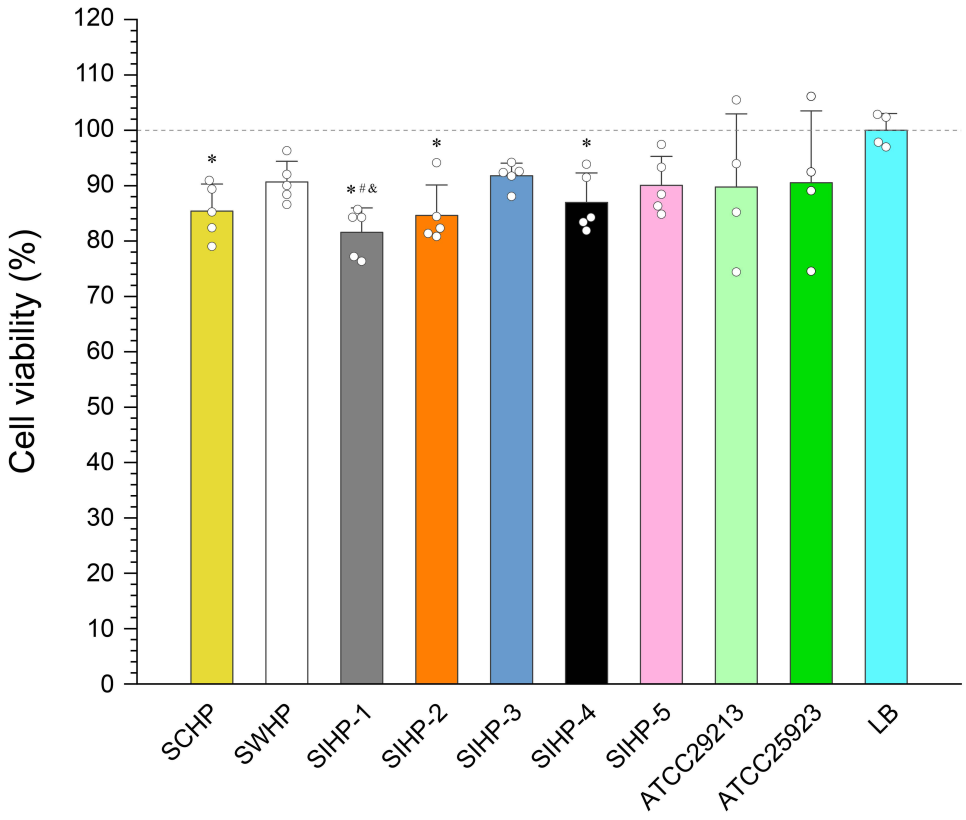

Figure 7 Cytotoxicity of *S. aureus* with different hemolytic phenotypes on RAW264.7 cells was evaluated by cell counting kit-8 (CCK8).
Notes: Bars indicate the standard deviations from the mean. *Statistically significant versus Luria-Bertani (LB) broth control; #Statistically significant versus *S. aureus* with weak hemolytic phenotype (SWHP); &Statistically significant versus *S. aureus* with incomplete hemolytic phenotype 3 (SIHP-3).

that acts as a master virulence transcriptional regulator.[29] To adapt quickly to changing conditions, *S. aureus* has evolved many different strategies for fine-tuning the expression of *agr*. Moreover, in the laboratory, spontaneous *agr* mutations have been frequently observed due to the high metabolic burden entailed by the *agr* autoactivation circuit.[30] *S. aureus* strains isolated from clinical samples often encounter host-immune system and sub-MICs of antibiotics. As environmental and host signals, they may trigger the virulence regulatory system of *S. aureus* and alter the expression of target genes. It has been demonstrated that *S. aureus* with nonhemolytic phenotype owing to mutations in *agr* or other loci during infection rather than subculturing after isolation,[20] although revertants have been found for 10% of clinical isolates.[31] Similarly, the emergence and discrepant microbiological characteristics of *S. aureus* strains with different hemolytic phenotypes in this study are most probably due to the same underlying reason.

Generally, the primary mechanisms of antibiotic resistance in *S. aureus* involve a variety of molecules including *blaZ*-encoded penicillinases, *mecA*-encoded penicillin-binding protein 2a (PBP2a), *mecC*-encoded PBP2c, *fem*-encoded enzymes related to cell wall synthesis, *llm*-encoded lipophilic membrane protein, *fmtA*-encoded penicillin-recognizing protein (PRP), and YsxC.[32–35] In the future, we plan to detect these antibiotic resistance-related genes in *S. aureus* with different hemolytic phenotypes, which will facilitate a more nuanced understanding of the genetic underpinnings of antibiotic resistance in this pathogenic bacterium, thereby informing the development of targeted therapeutic interventions.

Conclusion

Taken together, *S. aureus* with different hemolytic phenotypes have distinctive microbiological characteristics. Due to the difficulty in eliminating the irrational use of antibiotics, clinical microbiologists need to be vigilant about the hemolytic

phenotypes during the culture of *S. aureus* strains, and actively enhance communication with clinicians to optimize the treatment of infection.

Ethics Statement

S. aureus strains used in this study were previously isolated from clinical samples. There were no adverse reactions or risks to subjects. The Ethics Committee of Anhui Medical University approved this study (Approval number: LLSC20241798) but waived informed consent.

Data Sharing Statement

All data generated or analyzed during this study are included in this published article.

Acknowledgments

We especially thank Dr. Yang Li and Professor An Xu from the High Magnetic Field Laboratory, Hefei Institutes of Physical Science, Chinese Academy of Sciences, for their technical assistance.

Funding

This work was supported by the National Natural Science Foundation of China (grant number 82102460), the Clinical Research Cultivation Project of the Second Affiliated Hospital of Anhui Medical University (grant number 2021LCZD13), and the Natural Science Foundation of Anhui Medical University (grant number 2022xkj197).

Disclosure

The authors report no conflicts of interest in this work.

References

1. Antimicrobial Resistance Collaborators. Global burden of bacterial antimicrobial resistance in 2019: a systematic analysis. *Lancet*. 2022;399 (10325):629–655. doi:10.1016/S0140-6736(21)02724-0
2. Tong SY, Davis JS, Eichenberger E, Holland TL, VG F Jr. *Staphylococcus aureus* infections: epidemiology, pathophysiology, clinical manifestations, and management. *Clin Microbiol Rev*. 2015;28(3):603–661. doi:10.1128/CMR.00134-14
3. Lowy FD. Antimicrobial resistance: the example of *Staphylococcus aureus*. *J Clin Invest*. 2003;111(9):1265–1273. doi:10.1172/JCI18535
4. Zhang H, Zheng Y, Gao H, et al. Identification and characterization of *Staphylococcus aureus* strains with an incomplete hemolytic phenotype. *Front Cell Infect Microbiol*. 2016;6:146. doi:10.3389/fcimb.2016.00146
5. Yang H, Xu S, Huang K, et al. Anti-staphylococcus antibiotics interfere with the transcription of leucocidin ED gene in *Staphylococcus aureus* strain Newman. *Front Microbiol*. 2020;11:265. doi:10.3389/fmicb.2020.00265
6. Katahira EJ, Davidson SM, Stevens DL, Bolz DD. Subinhibitory concentrations of tedizolid potently inhibit extracellular toxin production by methicillin-sensitive and methicillin-resistant *Staphylococcus aureus*. *J Med Microbiol*. 2019;68(2):255–262. doi:10.1099/jmm.0.000905
7. Chen J, Zhou H, Huang J, Zhang R, Rao X. Virulence alterations in *Staphylococcus aureus* upon treatment with the sub-inhibitory concentrations of antibiotics. *J Adv Res*. 2021;31:165–175. doi:10.1016/j.jare.2021.01.008
8. Kernodle DS, McGraw PA, Barg NL, Menzies BE, Voladri RK, Harshman S. Growth of *Staphylococcus aureus* with nafcillin in vitro induces alpha-toxin production and increases the lethal activity of sterile broth filtrates in a murine model. *J Infect Dis*. 1995;172(2):410–419. doi:10.1093/infdis/172.2.410
9. Ohlsen K, Ziebuhr W, Koller KP, Hell W, Wichelhaus TA, Hacker J. Effects of subinhibitory concentrations of antibiotics on alpha-toxin (hla) gene expression of methicillin-sensitive and methicillin-resistant *Staphylococcus aureus* isolates. *Antimicrob Agents Chemother*. 1998;42 (11):2817–2823. doi:10.1128/AAC.42.11.2817
10. Worlitzsch D, Kaygin H, Steinhuber A, Dalhoff A, Botzenhart K, Döring G. Effects of amoxicillin, gentamicin, and moxifloxacin on the hemolytic activity of *Staphylococcus aureus* in vitro and in vivo. *Antimicrob Agents Chemother*. 2001;45(1):196–202. doi:10.1128/AAC.45.1.196-202.2001
11. Goerke C, Köller J, Wolz C. Ciprofloxacin and trimethoprim cause phage induction and virulence modulation in *Staphylococcus aureus*. *Antimicrob Agents Chemother*. 2006;50(1):171–177. doi:10.1128/AAC.50.1.171-177.2006
12. Williams RE, Harper GJ. Staphylococcal haemolysins on sheep-blood agar with evidence for a fourth haemolysin. *J Pathol Bacteriol*. 1947;59(1–2):69–78. doi:10.1002/path.1700590109
13. Haque RU, Baldwin JN. Types of hemolysins produced by *Staphylococcus aureus*, as determined by the replica plating technique. *J Bacteriol*. 1964;88(5):1442–1447. doi:10.1128/jb.88.5.1442-1447.1964
14. Gao M, Sang R, Wang G, Xu Y. Association of *pvl* gene with incomplete hemolytic phenotype in clinical *Staphylococcus aureus*. *Infect Drug Resist*. 2019;12:1649–1656. doi:10.2147/IDR.S197167
15. Atalla H, Gyles C, Mallard B. *Staphylococcus aureus* small colony variants (SCVs) and their role in disease. *Anim Health Res Rev*. 2011;12 (1):33–45. doi:10.1017/S1466252311000065
16. Green MR, Sambrook J. Precipitation of RNA with ethanol. *Cold Spring Harb Protoc*. 2020;2020(3):101717. doi:10.1101/pdb.prot101717

17. Bernal-Bayard J, Thiebaud J, Brossaud M, et al. Bacterial capsular polysaccharides with antibiofilm activity share common biophysical and electrokinetic properties. *Nat Commun*. 2023;14(1):2553. doi:10.1038/s41467-023-37925-8
18. Tang J, Kang M, Chen H, et al. The staphylococcal nuclease prevents biofilm formation in *Staphylococcus aureus* and other biofilm-forming bacteria. *Sci China Life Sci*. 2011;54(9):863–869. doi:10.1007/s11427-011-4195-5
19. Hu X, Jiang S, Xu F, et al. Engineering and functional analysis of yeast with a monotypic 40S ribosome subunit. *Proc Natl Acad Sci U S A*. 2022;119(6):e2114445119. doi:10.1073/pnas.2114445119
20. Traber KE, Lee E, Benson S, et al. *agr* function in clinical *Staphylococcus aureus* isolates. *Microbiology*. 2008;154(Pt 8):2265–2274. doi:10.1099/mic.0.2007/011874-0
21. Atalla H, Gyles C, Jacob CL, Moisan H, Malouin F, Mallard B. Characterization of a *Staphylococcus aureus* small colony variant (SCV) associated with persistent bovine mastitis. *Foodborne Pathog Dis*. 2008;5(6):785–799. doi:10.1089/fpd.2008.0110
22. Wang LJ, Yang X, Qian SY, et al. Identification of hemolytic activity and hemolytic genes of methicillin-resistant *Staphylococcus aureus* isolated from Chinese children. *Chin Med J*. 2020;133(1):88–90. doi:10.1097/CM9.0000000000000571
23. Rohmer C, Wolz C. The role of *hlb*-converting bacteriophages in *Staphylococcus aureus* host adaption. *Microb Physiol*. 2021;31(2):109–122. doi:10.1159/000516645
24. Aarestrup FM, Larsen HD, Eriksen NH, Elsberg CS, Jensen NE. Frequency of alpha- and beta-haemolysin in *Staphylococcus aureus* of bovine and human origin. A comparison between pheno- and genotype and variation in phenotypic expression. *APMIS*. 1999;107(4):425–430. doi:10.1111/j.1699-0463.1999.tb01576.x
25. Salgado-Pabón W, Herrera A, Vu BG, et al. *Staphylococcus aureus* β-toxin production is common in strains with the β-toxin gene inactivated by bacteriophage. *J Infect Dis*. 2014;210(5):784–792. doi:10.1093/infdis/jiu146
26. Hayashida A, Bartlett AH, Foster TJ, Park PW. *Staphylococcus aureus* beta-toxin induces lung injury through syndecan-1. *Am J Pathol*. 2009;174(2):509–518. doi:10.2353/ajpath.2009.080394
27. Katayama Y, Baba T, Sekine M, Fukuda M, Hiramatsu K. Beta-hemolysin promotes skin colonization by *Staphylococcus aureus*. *J Bacteriol*. 2013;195(6):1194–1203. doi:10.1128/JB.01786-12
28. Jenul C, Horswill AR. Regulation of *Staphylococcus aureus* virulence. *Microbiol Spectr*. 2018;6(1):GPP3–0031–2018. doi:10.1128/microbiolspec.GPP3-0031-2018
29. Raghuram V, Alexander AM, Loo HQ, Petit RA 3rd, Goldberg JB, Read TD. Species-wide phylogenomics of the *Staphylococcus aureus agr* operon revealed convergent evolution of frameshift mutations. *Microbiol Spectr*. 2022;10(1):e0133421. doi:10.1128/spectrum.01334-21
30. Novick RP, Geisinger E. Quorum sensing in staphylococci. *Annu Rev Genet*. 2008;42:541–564. doi:10.1146/annurev.genet.42.110807.091640
31. Gor V, Hoshi M, Takemura AJ, et al. Virulence reversion in *Staphylococcus aureus*. *Proceedings Of The Academy Of Natural Sciences Of Philadelphia*. 2021;66:24. doi:10.3390/proceedings2020066024.
32. Kumari R, Dalal V. Identification of potential inhibitors for LLM of *Staphylococcus aureus*: structure-based pharmacophore modeling, molecular dynamics, and binding free energy studies. *J Biomol Struct Dyn*. 2022;40(20):9833–9847. doi:10.1080/07391102.2021.1936179
33. Dalal V, Kumar P, Rakhaminov G, et al. Repurposing an ancient protein core structure: structural studies on FmtA, a novel esterase of *Staphylococcus aureus*. *J Mol Biol*. 2019;431(17):3107–3123. doi:10.1016/j.jmb.2019.06.019
34. Dalal V, Dhankhar P, Singh V, et al. Structure-based identification of potential drugs against FmtA of *Staphylococcus aureus*: virtual screening, molecular dynamics, MM-GBSA, and QM/MM. *Protein J*. 2021;40(2):148–165. doi:10.1007/s10930-020-09953-6
35. Kumari R, Rathi R, Pathak SR, Dalal V. Structural-based virtual screening and identification of novel potent antimicrobial compounds against YsxC of *Staphylococcus aureus*. *J Mol Struct*. 2022;1255. doi:10.1016/j.molstruc.2022.132476